Pramana – J. Phys., Vol. 37, No. 3, September 1991, pp. 281–292. © Printed in India.

Decoupling potentials for the three-body final state Schrödinger equation of knockout reactions

ARUN K JAIN

Nuclear Physics Division, Bhabha Atomic Research Centre, Bombay 400085, India

MS received 8 April 1991

Abstract. In the conventional distorted wave impulse approximation (DWIA) approach the three-body final state of a knockout reaction is decoupled by assuming a plane wave form for the coupling term. The influence of this decoupling approximation on the analyses of cluster knockout reactions has been investigated for a test case where the exact solution is obtainable. A proper treatment of the coupling term causes large oscillations in the effective distorting optical potentials for the decoupled Schrödinger equation. These decoupling potentials depend strongly not only on the partial wave angular momentum, l but also on their azimuthal projection, m.

Keywords. Three-body decoupled equation; distorted wave impulse approximation.

PACS Nos 24·50; 24·10

1. Introduction

Knockout reactions with coincident detection of two of the 3-particles in the final state have yielded a vast amount of data (Roos 1984; Chant 1978). Analyses of these data have provided many empirical deductions such as the applicability of the factorized impulse approximation (Gaillard *et al* 1970; Watson *et al* 1976; Roos *et al* 1969, 1976, 1977; Pugh *et al* 1969 and Jain *et al* 1973), the final state prescription (Pugh *et al* 1969; Gaillard *et al* 1970; Jain *et al* 1973), the assignment of orbital angular momentum for the bound state etc. There has however been some uncertainty regarding the momentum distribution (Jain and Sarma 1974, 1979) and the relative spectroscopic factors of the bound cluster states (Wang *et al* 1980). Besides this there exists a much larger discrepancy in the absolute spectroscopic factors (Grossiord *et al* 1977; Jain and Sarma 1979; Wang *et al* 1980; Chant *et al* 1978) for clustering derived from knockout reactions induced by different projectiles (Roos *et al* 1977; Wang *et al* 1980; Samanta *et al* 1982; Carey *et al* 1981). Due to the apparent dependence of clustering probabilities on the projectile the knockout reactions have lost not only much of their predictive power but also their credibility in terms of various deductions. In order to investigate the reasons for the discrepancy many of the approximations that go into the analyses of knockout reactions have been discussed in detail earlier (Chant and Roos 1977). Most of the conventional DWIA calculations (Chant and Roos 1977) use what is commonly known as kinematic coupling approximation (KCA) for separating the three-body final state Schrödinger equation into two 2-body Schrödinger equations. Recently in one investigation (Jain 1990), using an exactly solvable test case, it has been shown that the use of KCA causes a suppression of the surface contributions to the reaction matrix element even when weakly absorbing optical potentials are employed. The test case consists of a situation where out of the two distorting optical potentials one is absent.

It is of interest to know whether the contributions arising from the three-body coupling term can be taken care of by some modification of the distorting optical potentials. A detailed analysis of the influence and localization of the three-body coupling contributions and investigation of the nature of modifications required to effectively change the distorting optical potentials so as to reproduce the decoupled solution is the subject matter discussed in this paper. The analysis could become feasible because of the availability of the exactly solvable (Jain 1990) test case where one knows the solution of the three-body final state exactly in one particular coordinate system. This solution is much closer to the actual situation for $(e, e'x)$, (p, pd), (p, pt) and $(p, p\alpha)$ type of reactions where one of the three final state particles is relatively weakly interacting than for the $(\alpha, 2\alpha)$ type of reactions. Even though the discrepancy (Samanta *et al* 1982) between the ratio of DWIA (with KCA) prediction and corresponding experimental data for the (p, px) type of reactions is one or two orders of magnitude less than that for $(\alpha, \alpha x)$ type it has been found (Jain 1990) that in general the three-body coupling term requires particular attention. In fact it has been shown (Jain 1990) that the data on $^{16}O(p, p\alpha)^{12}C$ reaction at around 100 MeV could be explained by using the exact three-body final state test case wave functions only when one considers that not only protons but the α-particles also are not strongly absorbed by the residual ^{12}C nucleus. Support for the low absorption behaviour of proton, alpha and other nuclear particles by medium mass nuclei may however be sought from analysis of the behaviour of $(e, e'p)$ reaction (Geesaman *et al* 1989), anomalous large angle α-scattering (Brink *et al* 1978; Alam and Malik 1990) and the recent understanding of $^{12}C(^{12}C, ^{13}C)^{11}C$ reaction (Satchler 1989) through weakly attenuating optical potentials.

Under the circumstances of weak nuclear absorption the knockout reactions should have larger contributions both from the nuclear surface as well as the nuclear interior (Jain and Sarma 1979; Jain 1990). The three-body coupling term contributions to these reactions thus become all the more important and should be understood properly before drawing any conclusions from their analyses. For the test case, the three-body coupling term has been found to lead to effective local decoupling potentials which depend on orbital angular momentum, l as well as its azimuthal projections, m. These effective local decoupling potentials when used in place of conventional optical potentials in the final state Schrödinger equation will take care of the coupling term present in the test case situation. In § 2 formalism for the derivation of decoupling potentials from the exactly solvable test case is presented. A comparison of the resulting decoupling potentials with the input optical potentials for the 90 MeV $^{16}O(\alpha, 2\alpha)^{12}C_{gs}$ reaction as an example is presented and discussed in § 3. Conclusions are presented in § 4.

2. Formalism

The three-body final state Hamiltonian H_f for a knockout reaction $A(a, a'b)B$ is (Chant and Roos 1977)

$$H_f = H_a + H_b + H_B + T_a + T_b + T_B + V_{aB}(r_{aB}) + V_{bB}(r_{bB}). \tag{1}$$

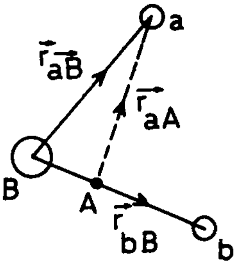

Figure 1. Relative coordinates $\mathbf{r}_{aB}$ and $\mathbf{r}_{bB}$ used for the kinematic coupling formalism and $\mathbf{r}_{aA}$ and $\mathbf{r}_{bB}$ used for the potential coupling formalism of the three-body final state treatment of $A(a, a'b)B$ knockout reaction.

Where H_x and T_x are respectively the internal Hamiltonian and kinetic energy operators for the x-th particle while V_{aB} and V_{bB} represent the interaction between $a-B$ and $b-B$ respectively which are commonly replaced by conventional distorting optical potentials. The impulse approximation takes care of the interaction $V_{ab}(r_{ab})$ and is thus not included as part of this final state Hamiltonian. This interaction, V_{ab} forms part of a factorization approximation where the matrix element of this interaction between initial and final scattering states is taken on-shell and is subsequently expressed in terms of observed cross section (Jackson and Berggren 1965). Re-expressing the final state Hamiltonian in terms of operators conjugate to relative coordinates $\mathbf{r}_{aB}$ and $\mathbf{r}_{bB}$ (see figure 1), one gets

$$H_f = H_a + H_b + H_B - \frac{\hbar^2}{2\mu_{aB}}\nabla^2_{aB} - \frac{\hbar^2}{2\mu_{bB}}\nabla^2_{bB} - \frac{\hbar^2}{m_B}\nabla_{aB}\cdot\nabla_{bB} + V_{aB}(r_{aB}) + V_{bB}(r_{bB}). \tag{2}$$

In the conventional DWIA calculations the coupling term $(-(\hbar^2/m_B)\nabla_{aB}\cdot\nabla_{bB})$ is approximated by its value in the plane wave limit or equivalently its asymptotic value $(=(\hbar^2/m_B)\mathbf{k}_{aB}\cdot\mathbf{k}_{bB})$. This approximation is commonly known as the kinematic coupling approximation (KCA) and as such it includes only the kinematic part of the coupling whereas the dynamical part is neglected in the Hamiltonian, H_f. This kinematic coupling approximation leads to a factorized scattering state wave function:

$$\Psi_f^{(-)}(\mathbf{r}_{aB}, \mathbf{r}_{bB}) \cong \chi_1^{(-)}(\mathbf{k}_{aB}, \mathbf{r}_{aB})\chi_2^{(-)}(\mathbf{k}_{bB}, \mathbf{r}_{bB}). \tag{3}$$

When in the Hamiltonian, H_f interaction potential $V_{aB}(r_{aB})$ is also not present then this solution reduces to

$$\Psi_{fT}^{(-)}(\mathbf{r}_{aB}, \mathbf{r}_{bB}) \cong \exp(i\mathbf{k}_{aB}\cdot\mathbf{r}_{aB})\chi_2^{(-)}(\mathbf{k}_{bB}, \mathbf{r}_{bB}). \tag{4}$$

This $\Psi_{fT}^{(-)}(\mathbf{r}_{aB}, \mathbf{r}_{bB})$ represents our test case wave function where $\mathbf{r}_{aB}$ and $\mathbf{r}_{bB}$ parts got separated due to KCA. Here

$$\mathbf{k}_{aB} = \mathbf{k}'_a - \frac{m_a}{(m_a + m_b + m_B)}\mathbf{k}_a, \quad \mathbf{k}_{bB} = \mathbf{k}_b - \frac{m_b}{(m_a + m_b + m_B)}\mathbf{k}_a, \tag{5}$$

with $\mathbf{k}_a$ being the incident wave vector of a and $\mathbf{k}'_a$, $\mathbf{k}_b$ and $\mathbf{k}_B$ representing the final state wave vectors of a, b and B respectively in the laboratory frame. Now consider a coordinate system where the relative coordinates are $\mathbf{r}_{aA}$ and $\mathbf{r}_{bB}$. The final state

Hamiltonian H_f in terms of operators conjugate to these relative coordinates is

$$H_f = H_a + H_b + H_B - \frac{\hbar^2}{2\mu_{aA}}\nabla^2_{aA} - \frac{\hbar^2}{2\mu_{bB}}\nabla^2_{bB} + V_{aB}(r_{aB}) + V_{bB}(r_{bB}). \tag{6}$$

In this representation of H_f the three-body coupling arises through the interaction $V_{aB}(r_{aB})$. For the test case where the potential $V_{aB}(r_{aB})$ goes to zero, the exact solution for this final state Hamiltonian, eq. (6) is

$$\Psi^{(-)}_{fT}(\mathbf{r}_{aA}, \mathbf{r}_{bB}) = \exp(i\mathbf{k}_{aA}\cdot\mathbf{r}_{aA})\chi^{(-)}_2(\mathbf{k}'_{bB}, \mathbf{r}_{bB}), \tag{7}$$

where

$$\mathbf{k}_{aA} = \mathbf{k}'_a - \frac{m_a}{(m_a + m_b + m_B)}\mathbf{k}_a, \quad \mathbf{k}'_{bB} = \frac{(m_B\mathbf{k}_b - m_b\mathbf{k}_B)}{(m_b + m_B)}. \tag{8}$$

since

$$\mathbf{k}_{aA} \equiv \mathbf{k}_{aB} \quad \text{and} \quad \mathbf{r}_{aA} = \mathbf{r}_{aB} - \frac{m_b}{(m_b + m_B)}\mathbf{r}_{bB}, \tag{9}$$

the exact test case wave function, eq. (7) can be written as:

$$\Psi^{(-)}_{fT}(\mathbf{r}_{aA}, \mathbf{r}_{bB}) = \exp(i\mathbf{k}_{aB}\cdot\mathbf{r}_{aB})\exp\left\{-i\frac{m_b}{(m_b + m_B)}\mathbf{k}_{aB}\cdot\mathbf{r}_{bB}\right\}\chi^{(-)}_2(\mathbf{k}'_{bB}, \mathbf{r}_{bB}). \tag{10}$$

From here one gets the $\mathbf{r}_{bB}$ part of the final state wave function for the test case exactly as:

$$\Psi^{(-)}_2(\mathbf{r}_{bB}) = \exp\left\{-i\frac{m_b}{(m_b + m_B)}\mathbf{k}_{aB}\cdot\mathbf{r}_{bB}\right\}\chi^{(-)}_2(\mathbf{k}'_{bB}, \mathbf{r}_{bB}) \tag{11}$$

in place of $\chi^{(-)}_2(\mathbf{k}_{bB}, \mathbf{r}_{bB})$ of (4) which has been obtained by using the KCA.

It is easy to verify that

$$\mathbf{k}_{bB} \equiv \mathbf{k}'_{bB} - \frac{m_b}{(m_b + m_B)}\mathbf{k}_{aB}, \tag{12}$$

which in the plane wave limit (when both V_{aB} and V_{bB} go to zero) leads to the same wave function from the two-coordinate representations, $(\mathbf{r}_{aB}, \mathbf{r}_{bB})$ and $(\mathbf{r}_{aA}, \mathbf{r}_{bB})$. It is evident now that when $m_B \gg m_b$ the exact test case wave function $\Psi^{(-)}_2(\mathbf{r}_{bB})$ will practically tend to the corresponding KCA wave function $\chi^{(-)}_2(\mathbf{k}_{bB}, \mathbf{r}_{bB})$ which is what one would anticipate because the coupling term contributions are small when m_B becomes large. Similarly when the other potential, $V_{bB}(r_{bB})$ also becomes small the KCA final state wave function, $\Psi^{(-)}_{fT}(\mathbf{r}_{aB}, \mathbf{r}_{bB})$ of (4) goes over to the exact wave function $\Psi^{(-)}_{fT}(\mathbf{r}_{aA}, \mathbf{r}_{bB})$ of (10) because of the identity eqs (8) and (12).

For comprehending the implications of the KCA, which is routinely employed for analyses of knockout reactions, a comparison of the $\mathbf{r}_{bB}$ part of the test case wave functions of (4) and (10) alone does not provide much insight. This insight is provided when we consider the $\mathbf{r}_{bB}$ parts of the wave functions of (4) and (10) as solutions of following equation:

$$\left[-\frac{\hbar^2}{2\mu_{bB}}\nabla^2_{bB} + V_{\text{eff}}(\mathbf{r}_{bB})\right]\Psi^{(-)}_2(\mathbf{r}_{bB}) = E_{bB}\Psi^{(-)}_2(\mathbf{r}_{bB}). \tag{13}$$

One sees that when $V_{\rm eff}(\mathbf{r}_{bB}) \Rightarrow V_{bB}(r_{bB})$ in (13) the KCA solution, $\chi_2^{(-)}(\mathbf{k}_{bB}, \mathbf{r}_{bB})$ of (4) is obtained. A condition can be found for $V_{\rm eff}(\mathbf{r}_{bB})$ such that the $\mathbf{r}_{bB}$ component of the test case wave function, $\Psi_2^{(-)}(\mathbf{r}_{bB})$ of (11) is a solution of (13).

Abbreviating $\{(m_b/(m_b + m_B)\}$ as ε and expanding $\exp(-i\varepsilon \mathbf{k}_{aB} \cdot \mathbf{r}_{bB})$ and $\chi_2^{(-)}(\mathbf{k}'_{bB}, \mathbf{r}_{bB})$ in terms of partial waves one gets (11) as:

$$\Psi_2^{(-)}(\mathbf{r}_{bB}) = (4\pi)^2 \sum_{l_1} i^{-l_1} j_{l_1}(\varepsilon k_{aB} r_{bB}) \sum_{m_1} Y_{l_1 m_1}(\hat{r}_{bB})\, Y^*_{l_1 m_1}(\hat{k}_{aB})$$
$$\times \sum_{l_2} i^{l_2} \frac{f_{l_2}(k'_{bB} r_{bB})}{k'_{bB} r_{bB}} \sum_{m_2} Y_{l_2 m_2}(\hat{r}_{bB})\, Y^*_{l_2 m_2}(\hat{k}'_{bB}). \tag{14}$$

Combining the spherical harmonics $Y_{l_1 m_1}(\hat{r}_{bB})$ and $Y_{l_2 m_2}(\hat{r}_{bB})$ into $Y_{lm}(\hat{r}_{bB})$ and comparing its coefficients with that corresponding to $Y_{lm}(\hat{r}_{bB})$ in the following

$$\Psi_2^{(-)}(\mathbf{r}_{bB}) = 4\pi \sum_{l,m} i^l \frac{f_{lm}(k_{bB} r_{bB})}{k_{bB} r_{bB}}\, Y_{lm}(\hat{r}_{bB})\, Y^*_{lm}(\hat{k}_{bB}), \tag{15}$$

one sees that

$$\frac{f_{lm}(k_{bB} r_{bB})}{(k_{bB} r_{bB})} = \sum_{l_1 l_2} G(l_1, l_2, l, m; \hat{k}_{aB}, \hat{k}_{bB})\, j_{l_1}(\varepsilon k_{aB} r_{bB}) \frac{f_{l_2}(k'_{bB} r_{bB})}{(k'_{bB} r_{bB})} \tag{16}$$

where

$$G(l_1, l_2, l, m; \hat{k}_{aB}, \hat{k}'_{bB}) = i^{l_2 - l_1 - l} \left(\frac{4\pi(2l_1 + 1)(2l_2 + 1)}{(2l + 1)} \right)^{1/2} C(l_1, l_2, l; 0, 0)$$
$$\times \sum_{m_1} C(l_1, l_2, l; m_1, (m - m_1))\, Y^*_{l_1 m_1}(\hat{k}_{aB})\, Y^*_{l_2 (m - m_1)}(\hat{k}'_{bB}). \tag{17}$$

The function $f_{lm}(k_{bB} r_{bB})$ of (16) satisfies the following radial equation:

$$\left(\frac{\mathrm{d}^2}{\mathrm{d}R^2} - \frac{l(l+1)}{R^2} - \frac{2\mu_{bB}}{\hbar^2} V^{l,m}_{\rm eff}(R) + k^2_{bB} \right) f_{lm}(k_{bB} R) = 0. \tag{18}$$

Knowledge of $f_{lm}(k_{bB} R)$ from (16) for various kinematic conditions (so that $\mathbf{k}_{aB}$ and $\mathbf{k}_{bB}$ are known) leads to effective local decoupling potentials, $V^{lm}_{\rm eff}(R)$ which give exact decoupled final state for the test case. These effective local decoupling potentials depend on the input optical potential, $V_{bB}(R)$ in the outgoing channel. Properties of the effective decoupling potentials for various input potentials as well as for different kinematic conditions are discussed in the next section.

3. Decoupling potentials, results and discussion

The solution of eq. (18), $f_{lm}(k_{bB} r_{bB})$ which incorporates the proper decoupling potentials, $V^{l,m}_{\rm eff}(r_{bB})$ describes the r_{bB} component of the three-body final state for the test case (where the $a - B$ channel potential, $V_{aB}(r_{aB})$ is zero). When the $b - B$ channel potential is also zero then, as expected, it has been found that the corresponding decoupling potentials, $V^{l,m}_{\rm eff}(r_{bB})$ go to zero and the solution of (18), $f_{lm}(k_{bB} r_{bB})/(k_{bB} r_{bB})$ becomes independent of the m-quantum number and transforms to corresponding

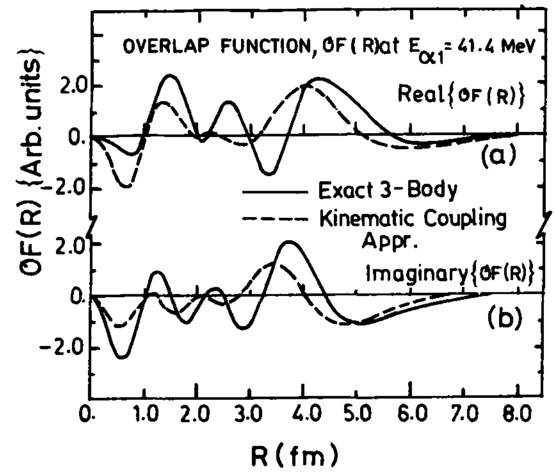

Figure 2. Overlap function, $OF(R)$ *vs.* intercluster $(\alpha - {}^{12}\mathrm{C})$ separation, R for 90 MeV kinematics of ${}^{16}\mathrm{O}(\alpha, 2\alpha){}^{12}C_{gs}$ reaction for zero recoil momentum position, $E_{\alpha 1} = 41{\cdot}423$ MeV using only the real part of the $\alpha - {}^{12}\mathrm{C}$ optical potential and no imaginary component, (**a**) real part and (**b**) imaginary part.

spherical Bessel function $j_l(k_{bB}r_{bB})$. For calculating effective decoupling potentials, $V_{\mathrm{eff}}^{l,m}(R)$ from (16) and (17) sums over l_1, l_2 and m_1 are to be performed. In order to perform calculations one is required to restrict the sum to finite values of l_1 and l_2 which contribute significantly (for the calculations presented as example of 90 MeV ${}^{16}\mathrm{O}(\alpha, 2\alpha){}^{12}\mathrm{C}_{gs}$ reaction here the maximum values have been restricted to 22 for each of them). Decoupling potentials have been evaluated for l-values between 0 and 10. Due to the use of limited values of l_1 and l_2 inaccuracies are expected to occur in the calculated values of $V_{\mathrm{eff}}^{l,m}(R)$ for large R's where larger l_1's and l_2's predominantly contribute. Behaviour of the overlap functions seen here in figure 2 (and also in Jain 1990), a comparison of the exact and kinematic coupling approximation results shows that the two differ significantly even at larger R's ($R \geqslant 3$ fm). This indicates that the $V_{\mathrm{eff}}^{l,m}(R)$ should be much different from the input $V_{bB}(R)$ even for larger l's. At smaller R's however, amplitudes of the wave functions corresponding to larger partial waves are small and have larger inaccuracies leading to inaccurate $V_{\mathrm{eff}}(R)$ at these small R's. Decoupling potentials, however, are expected to be reasonably accurate at intermediate R-values.

The 90 MeV ${}^{16}\mathrm{O}(\alpha, 2\alpha){}^{12}\mathrm{C}_{gs}$ reaction serves as an example to investigate the general behaviour of the decoupling potentials. A comparison of the KCA and the exact treatment of the three-body coupling term for this example is seen in figures 2 and 3 for the overlap function and cross section respectively (see Jain 1990). It is evident that the conventional use of $V_{bB}(R)$ of the KCA in place of $V_{\mathrm{eff}}^{l,m}(R)$ of the exact treatment makes a dramatic difference. For some representative l-values ($l = 0, 3$ and 6) and corresponding permissible m-values $V_{\mathrm{eff}}^{l,m}(R)$ values are plotted as a function of R in figures 4–6 where the imaginary part of the input potential is taken as zero. One of the striking features observed in these plots is sharp peaks and dips in the $V_{\mathrm{eff}}^{l,m}(R)$ as a function of R. Besides this different m-values are seen to have differences in spikes and dips in these plots in contrast to the smooth behaviour of the input optical potential, $V_{\alpha - {}^{12}\mathrm{C}}(R)$. Even when the input optical potential is purely real the $V_{\mathrm{eff}}^{l,m}(R)$

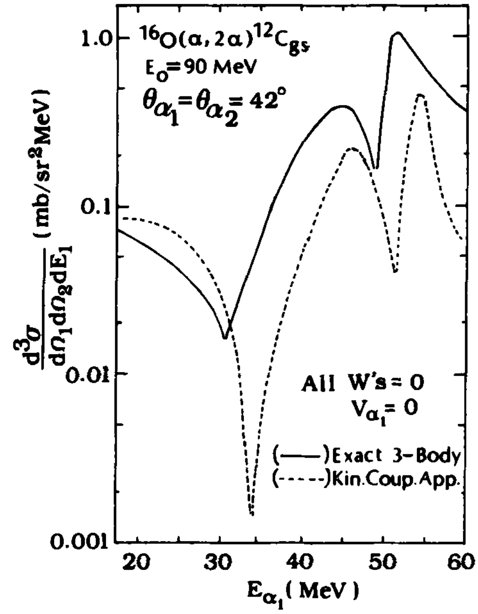

Figure 3. Calculated energy sharing distribution for 90 MeV $^{16}O(\alpha, 2\alpha)$ reaction kinematics for the test case when $V_{\alpha 1 - ^{12}C}$ optical potential is taken as zero for the final state and all imaginary components are neglected, (———) exact three body coupling, and (– – –) conventional KCA.

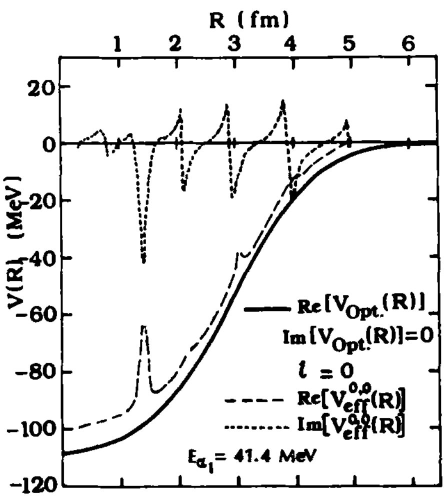

Figure 4. Comparison of the decoupling potentials, $V^{l,m}_{eff}(R)$ with the corresponding input optical potential, $V_{opt}(R)$ when $l = 0$ for the 90 MeV $^{16}O(\alpha, 2\alpha)^{12}C_{gs}$ reaction at $E_{\alpha 1}$ (energy of the outgoing α which is not interacting with the residual ^{12}C nucleus) = 41·4 MeV when the imaginary part of $V_{opt}(R)$ is taken to be zero.

has been found to have substantial imaginary component. The spikes and dips in the $V^{l,m}_{eff}(R)$ are seen to oscillate around the average input optical potential, $V_{\alpha - ^{12}C}(R)$. The imaginary component of $V^{l,m}_{eff}(R)$ itself has large variations from positive to negative and vice versa indicating a corresponding redistribution (enhancement or

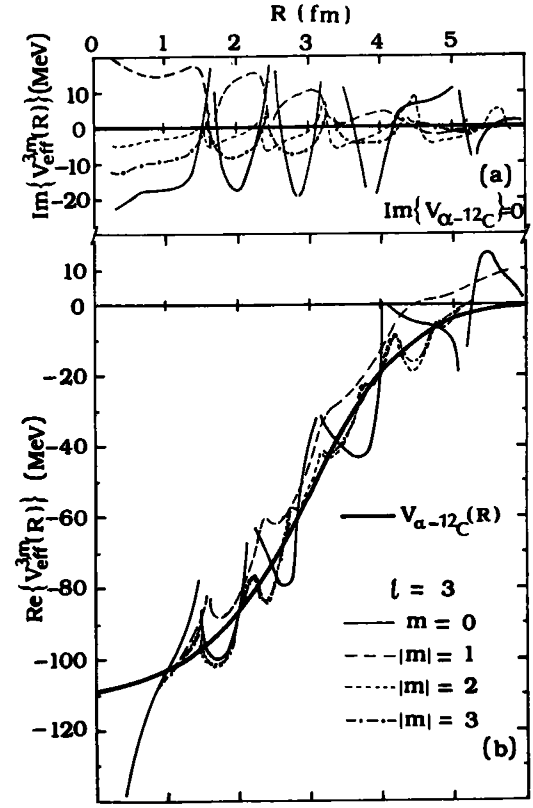

Figure 5. Same as for figure 4 except that here it is for $l = 3$ (**a**) imaginary part of the potential and, (**b**) real part of the potential.

attenuation) of the wave function. Enhancement of $OF(R)$ in figure 2 for values of R in the range $\approx 1{\cdot}5$ to $\approx 3{\cdot}5$ fm arises because the partial waves peaking in this zone are enhanced due to the effective decoupling potentials.

Large differences between $V_{\text{eff}}^{l,m}(R)$ and $V_{bB}(R)$ indicate that the effect of the coupling term is large and peaks in the surface region of the nucleus. The form of $V_{\text{eff}}^{l,m}(R)$ as a function of R changes as the energy in this channel is changed. This can be seen when the effective decoupling potentials for $l = 0$, shown in figures 7 and 4 at energies, $E_{\alpha 1} = 51{\cdot}5$ and $41{\cdot}4$ MeV respectively are compared with each other. The wide ranging oscillations in $V_{\text{eff}}^{l,m}(R)$ arise mainly because the zeros of the double derivative of $f_{lm}(k_{bB}R)$ do not coincide with the zeros of itself. Due to this reason the dramatic variations in the effective decoupling potentials observed in this representative example do not seem to be obtainable through any general law or systematics.

Behaviour of the effective decoupling potentials, $V_{\text{eff}}^{l,m}(R)$ for a case when the usual complex input optical potential is used can be observed in figures 8 and 9 for $l = 3$ and 6 respectively at $E_{\alpha 1} = 41{\cdot}4$ MeV. These $V_{\text{eff}}^{l,m}(R)$ are seen to have less strong oscillations for lower partial waves but they become strong for larger l-values. It is our endeavour to see if the decoupled wave functions or the effective decoupling potentials can be made use of in analysing the existing knockout reaction data and hence explain the orders of magnitude discrepancies in understanding the $(\alpha, \alpha x)$ type of reactions.

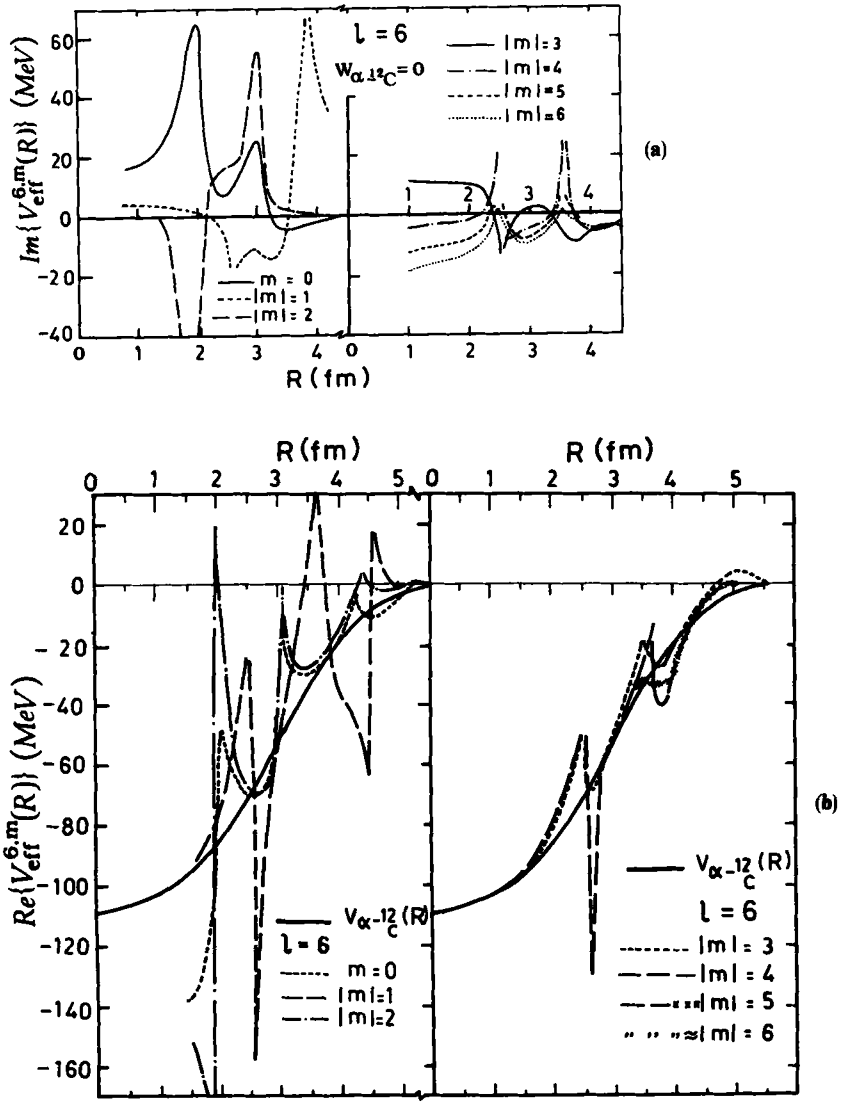

Figure 6. Same as figure 4 except that it is for $l = 6$, (**a**) imaginary part of the potential and, (**b**) real part of the potential.

4. Conclusions

Through the effective decoupling potentials obtained from the test case situation one can exactly simulate the contributions arising from the three-body coupling term. Generally these effective decoupling potentials, $V_{\rm eff}^{l,m}(R)$ are seen to have strong oscillations as a function of R. The behaviour of these effective decoupling potentials also changes dramatically not only with the change of l-value but also with its z-projection, m. Enhancement of the knockout reaction cross-section is seen to be large from the surface region of the nucleus only when the attenuation due to the imaginary component of the optical potential is weak. This observation increases the

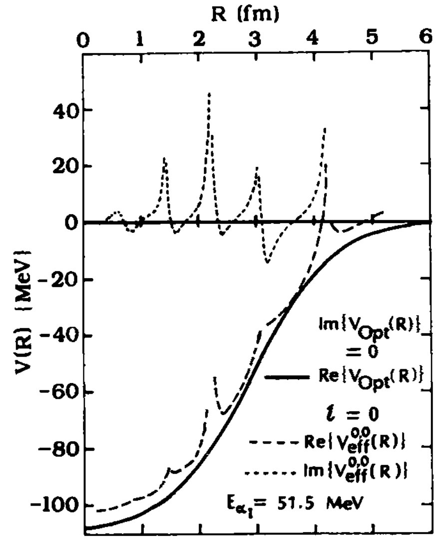

Figure 7. Same as for figure 4 except that here it is for $E_{\alpha 1} = 51{\cdot}5$ MeV.

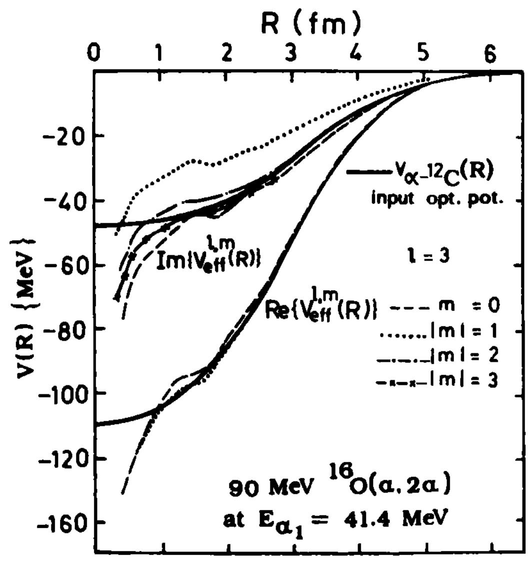

Figure 8. Same as for figure 4 except that here it is for complex input optical potential and for $l = 3$.

importance of the three-body coupling term particularly when validity of recently obtained weakly attenuating optical potentials (Geesaman *et al* 1989; Brink *et al* 1978; Alam and Malik 1990; Satchler 1989) is to be believed strongly. The present understanding (Jain and Sarma 1979; Jain 1990) of the knockout reactions in terms of DWIA tends to support the use of weakly attenuating optical potentials. Use of decoupled test case wave functions or the corresponding effective decoupling potentials for the analyses of $(\alpha, \alpha x)$ reactions is yet to be worked out.

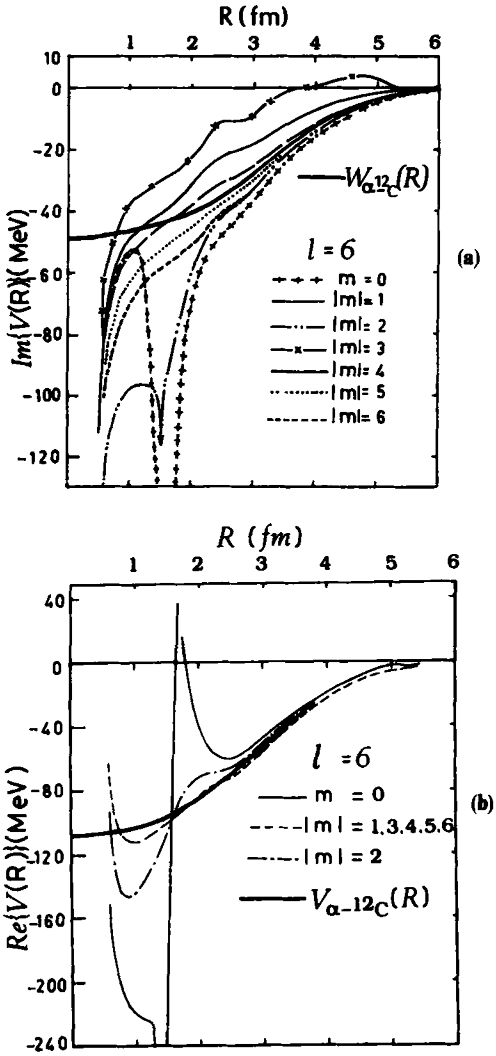

Figure 9. Same as for figure 4 except that here it is for complex input optical potential as also for figure 8 but for $l = 6$, (a) imaginary part of the potential and, (b) real part of the potential.

Acknowledgements

The author would like to thank Dr N Sarma for helpful discussions and critical reading of the manuscript on this work and Dr Amit Roy for computational support during various stages of development of the formalism and computer program.

References

Alam M M and Malik F B 1990 *Phys. Lett.* **B237** 14
Brink D M, Grabowski J and Vogt E 1978 *Nucl. Phys.* **A309** 359

Carey T A, Roos P G, Chant N S, Nadasen A and Chen H L 1981 *Phys. Rev.* **C23** 576
Carey T A, Roos P G, Chant N S, Nadasen A and Chen H L 1984 *Phys. Rev.* **C29** 1273
Chant N S and Roos P G 1977 *Phys. Rev.* **C15** 57
Chant N S 1978 *Proc. 3rd Int. Conf. on clustering aspects of Nucl. structure and Nucl. reactions*, Winnipeg, Manitoba, p. 415 and references therein
Chant N S, Roos P G and Wang C W 1978 *Phys. Rev.* **C17** 8
Gaillard P, Chevallier M, Grossiord J Y, Guichard A, Gusakow M and Pizzi J R 1970 *Phys. Rev. Lett.* **25** 593
Geesaman *et al* 1989 *Phys. Rev. Lett.* **63** 734
Grossiord J Y, Bedjidian M, Guichard A, Gusakow M, Pizzi J R, Delbar T, Gregoire G and Lega J 1977 *Phys. Rev.* **C15** 843
Jackson D F and Berggren T 1965 *Nucl. Phys.* **62** 353
Jain A K, Grossiord J Y, Chevallier M, Gaillard P, Guichard A, Gusakow M and Pizzi J R 1973 *Nucl. Phys.* **A216** 519
Jain A K and Sarma N 1974 *Nucl. Phys.* **A233** 145
Jain A K and Sarma N 1979 *Nucl. Phys.* **A321** 429
Jain A K 1990 *Phys. Rev.* **C42** 368
Pugh H G, Watson J W, Goldberg D A, Roos P G, Bonbright D I and Riddle R A J 1969 *Phys. Rev. Lett.* **22** 408
Roos P G, Kim H, Jain M and Holmgren H D 1969 *Phys. Rev. Lett.* **22** 242
Roos P G, Goldberg D A, Chant N S, Woody R III and Reichart W 1976 *Nucl. Phys.* **A257** 317
Roos P G, Chant N S, Cowley A A, Goldberg D A, Holmgren H D and Woody R 1977 *Phys. Rev.* **C15** 69
Roos P G 1984 *in Proc. of Int. Conf. on clustering aspects of Nucl. Struct. and Nucl. reactions*, Chester (UK) p. 279, and references therein
Samanta C, Chant N S, Roos P G, Nadasen A and Cowley A A 1982 *Phys. Rev.* **C26** 1379
Satchler G R 1989 *Nucl. Phys.* **A505** 103
Wang C W, Chant N S, Roos P G, Nadasen A, and Carey T A 1980 *Phys. Rev.* **C21** 1705
Watson J W, Pugh H G, Roos P G, Goldberg D A, Riddle R A J and Bonbright D I 1976 *Nucl. Phys.* **A172** 317